AD-A088 083 NAVAL RESEARCH LAB WASHINGTON DC F/G 20/4
VORTEX SHEDDING FROM STATIONARY AND VIBRATING BLUFF BODIES IN A--ETC(U)
AUG 80 O M GRIFFIN
UNCLASSIFIED NRL-MR-4287 NL

NRL Memorandum Report 4307

Vortex Shedding From Stationary and Vibrating Bluff Bodies in a Shear Flow

Owen M. Griffin

Marine Technology Division

(12) LEVEL II

August 11, 1980

NAVAL RESEARCH LABORATORY
Washington, D.C.

SECURITY CLASSIFICATION OF THIS PAGE (When Data Entered)

REPORT DOCUMENTATION PAGE

READ INSTRUCTIONS BEFORE COMPLETING FORM

1. REPORT NUMBER: NRL Memorandum Report 4287
2. GOVT ACCESSION NO.: AD-A088 083
3. RECIPIENT'S CATALOG NUMBER:

4. TITLE (and Subtitle): VORTEX SHEDDING FROM STATIONARY AND VIBRATING BLUFF BODIES IN A SHEAR FLOW
5. TYPE OF REPORT & PERIOD COVERED: Interim, FY 1980
6. PERFORMING ORG. REPORT NUMBER:

7. AUTHOR(s): Owen M. Griffin
8. CONTRACT OR GRANT NUMBER(s):

9. PERFORMING ORGANIZATION NAME AND ADDRESS: Naval Research Laboratory, Washington, D.C. 20375
10. PROGRAM ELEMENT, PROJECT, TASK AREA & WORK UNIT NUMBERS: NCBC, PO-4-0009; 0274-0-0

11. CONTROLLING OFFICE NAME AND ADDRESS: Civil Engineering Laboratory, Naval Construction Battalion Center, Port Hueneme, CA 93043
12. REPORT DATE: August 1980
13. NUMBER OF PAGES: 42

14. MONITORING AGENCY NAME & ADDRESS (if different from Controlling Office): NRL-MR-4287
15. SECURITY CLASS. (of this report): UNCLASSIFIED
15a. DECLASSIFICATION/DOWNGRADING SCHEDULE:

16. DISTRIBUTION STATEMENT (of this Report)

Approved for public release; distribution unlimited.

17. DISTRIBUTION STATEMENT (of the abstract entered in Block 20, if different from Report)

DTIC ELECTE S AUG 19 1980 D B

18. SUPPLEMENTARY NOTES

19. KEY WORDS (Continue on reverse side if necessary and identify by block number)

Vortex shedding
Vortex-excited oscillations
Ocean Engineering
Wind Engineering

20. ABSTRACT (Continue on reverse side if necessary and identify by block number)

If a fluid is in relative motion past a stationary bluff, or unstreamlined, structure and the vortex shedding frequency approaches one of the natural frequencies of the structure, then resonant flow-induced oscillations of the structure can occur when the damping of the system is sufficiently low. These resonant oscillations are accompanied by a 'lock-on' or capture of the vortex shedding frequency by the vibration frequency over a range of flow speeds, and this lock-on effect causes the wake and the structure to oscillate in unison. The periodic lift and the mean drag forces are amplified as a result of the vibrations, and changes in these fluid forces are closely

(Continued)

DD FORM 1 JAN 73 1473 EDITION OF 1 NOV 55 IS OBSOLETE S/N 0102-014-6601

251950

20; Abstract (Continued)

related to the changes that occur in the flow field in the near wake of the body. Many practical ocean and wind engineering situations involve lightly-damped structures that are located in flows of air or water that are nonuniform along the length of the structure. The primary difference between a uniform flow and a shear flow is the presence and added complexity, in a shear flow, of vorticity whose vector is normal to the plane of the flow. When the incident flow approaches the body this vorticity is turned into the flow direction and interacts with the vortices which are shed from the body into the wake.

The purpose of this report is to examine the general problem of the flow about bluff bodies in a shear flow in light of the present state of knowledge for these flows, and to relate existing studies to problems concerning the vortex-excited oscillations of long flexible structures in air and in water. Experiments conducted with cylinders of circular cross-section are emphasized, although reference is also made to experiments conducted with cylinders of other cross-sections (D-section cylinders, rectangular cylinders, etc.).

CONTENTS

1. INTRODUCTION 1

2. A SUMMARY OF RELATED INVESTIGATIONS 2

3. THE CHARACTERISTICS OF SHEAR FLOW PAST STATIONARY BLUFF BODIES 5

4. THE EFFECTS OF BODY OSCILLATIONS 11

5. METHODS FOR ESTIMATING THE BOUNDS OF FREQUENCY LOCK-ON IN A SHEAR FLOW 14

6. CONCLUDING REMARKS 16

7. REFERENCES 18

8. APPENDIX 22

I. Methods for Estimating the Susceptibility of Bluff Bodies to Cross Flow Vortex-Excited Oscillations 22

VORTEX SHEDDING FROM STATIONARY AND VIBRATING BLUFF BODIES IN A SHEAR FLOW

1. INTRODUCTION

If a fluid is in relative motion past a stationary bluff, or unstreamlined, structure and the vortex shedding frequency approaches one of the natural frequencies of the structure, then resonant flow-induced oscillations of the cylinder can occur when the damping of the system is sufficiently low. These resonant oscillations are accompanied by a 'lock-on' or capture of the vortex shedding frequency by the vibration frequency over a range of flow speeds, and this lock-on effect causes the wake and the structure to oscillate in unison. The periodic lift and the mean drag forces are amplified as a result of these vibrations, and changes in these fluid forces are closely related to the changes that occur in the flow field in the near wake of the body. Many practical situations involve lightly-damped structures that are located in flows of air or water that are nonuniform along the length of the structure. The primary difference between a uniform flow and a shear flow is the presence and added complexity, in a shear flow, of vorticity whose vector is normal to the plane of the flow. When the incident flow approaches the body this vorticity is turned into the flow direction and it interacts with the vortices which are shed from the body into the wake.

The complex fluid-structure interaction associated with vortex shedding from a bluff body in a nonuniform (shear) flow encompasses a wide range of problems. For instance, tall buildings of various cross-sections and slenderness or aspect ratios, i.e., length L/diameter D, often pose difficult and varied problems to the structural designer and architect. These problems include flow-induced structural fatigue and interactions between the structure and the atmospheric boundary layer. Cylindrical structures such as these are of finite length with a relatively small aspect ratio (L/D = 2 to 15). On the other hand, structures intended for deployment in the ocean range from small aspect-ratio bluff bodies such as marine pilings in shallow water to long cable arrays with aspect ratios of several hundred, to long marine risers, and to pipelines. The cold water intake pipe of an ocean thermal energy conversion (OTEC) power plant also is a long, cylindrical structure deployed in an often nonuniform current field.

Manuscript submitted May 27, 1980.

Ocean currents typically vary vertically and horizontally in both shallow and deep water, so that nonuniform flow effects may need to be given serious consideration by the designer of marine structures.

The purpose of this report is to examine the general problem of the flow about bluff bodies in a shear flow in light of the present state of knowledge for these flows, and to relate existing studies to the vortex-excited oscillations of slender, flexible structures in air and in water. Experiments with circular cylinders are emphasized, although reference also is made to experiments conducted with cylinders of other cross-sections (D-section cylinders, rectangular cylinders, etc.).

2. RELATED INVESTIGATIONS

A number of papers which treat various aspects of unsteady flow phenomena and, in particular, the vortex-excited oscillations of bluff bodies and the equivalent forced vibrations have recently appeared. These include the proceedings of two international symposia on flow-induced structural vibrations (1,2), which contain papers ranging from basic laboratory and analytical studies of vortex formation in uniform and nonuniform flows to field studies of the vibrations of offshore structures. Research into unsteady flow phenomena through 1976 was reviewed by McCroskey (3), and Sarpkaya (4) has reviewed in detail the problems associated with vortex-excited oscillations and has provided one hundred and thirty-four references through early 1979.

Vortex-excited oscillations are a complex phenomenon when the incident flow to the structure is uniform and steady, but they are even more complex when the structure is at yawed incidence and/or the flow is nonuniform. The former problem of flow at yawed incidence was studied recently by Ramberg (5), and the latter problem is discussed here. In an early study of shear flow past bluff bodies, Masch and Moore (6) undertook an experimental investigation of the drag force variation on cylinders in the presence of a linear velocity profile at incidence; up to 40 percent deviations from the uniform flow values of the drag coefficient were measured in the case of the linear velocity profile. Visualization of the flow in the wake showed the presence of appreciable secondary flow effects due to the velocity gradient. Starr (7) and Shaw and Starr (8) measured the flow about and the force distribution on circular cylinders in nonuniform flows of water and air. These studies showed the potential importance of characterizing the nonuniform flow in terms of a "steepness parameter" for the incident velocity gra-

dient. Both studies were mainly concerned with identifying design guidelines for use in engineering practices. The steepness parameter is defined by

$$\bar{\beta} = \frac{D}{V_{REF}} \frac{dV}{d\bar{z}} \tag{1}$$

where the velocity gradient is given by $dV/d\bar{z}$ and the cylinder diameter or representative transverse dimension by D. The reference velocity V_{REF} is usually representative of the mid-span incident velocity on a finite-length body or is equal to the velocity at the center of the wind tunnel or flow channel. Sometimes the maximum velocity in the profile is used to define V_{REF}.

A number of investigators have attempted to study nonuniform flow effects from a basic perspective. These studies have included the measurement of the base pressure and vortex shedding characteristics on D-shaped models which span the working section of a wind tunnel (9, 10, 11), base pressure and vortex shedding from finite-length circular cylinders (12), circular cylinders spanning a wind tunnel section (11) and rectangular cylinders of various aspect ratios in low and high turbulence level incident flows (13,14). Stansby (15) has measured the vortex shedding characteristics of circular cylinders which spanned the working section of a wind tunnel both in uniform flow and in an incident linear velocity gradient. The cylinder was forced to vibrate at various frequencies and amplitudes and the bounds for the 'lock-on' of the vortex shedding to the cylinder vibrations were measured for both uniform and nonuniform incident velocity profiles.

Vickery and Clark (16) studied the structure of the vortex shedding from a slender, tapered circular cylinder in smooth and turbulent shear flows. A three-celled shedding pattern was observed in the smooth uniform flow over the free-ended cylinder with a taper of 4 percent along its length. When the smooth flow was replaced by a turbulent shear flow, the vortex shedding cells of constant frequency were less apparent. The shedding frequency in this latter case varied continuously along the lower two-thirds of the cylinder, but two cell-like regions of constant frequency were present over the upper third.

The effect of a sheared turbulent stream on the critical Reynolds number for a circular cylinder was studied recently by Davies (17). The effect of the highly turbulent shear flow ($\bar{\beta} = 0.18$) was to

reduce the critical Reynolds number by a factor of ten, from Re_{crit} (smooth flow) = 2 to 3 × 10^5 to $Re_{crit} \approx 3 \times 10^4$. The overall effect was similar to that produced by a highly turbulent uniform flow of the same intensity ($v'/V \approx 5\%$). Once again a cellular vortex structure was observed along the span of the cylinder and the character and extent of each vortex shedding cell was dependent on local conditions and on the cylinder's relatively small aspect ratio, L/D = 6.

Stansby (15) has developed an approximate method for estimating the spanwise extent to which the vortex shedding locks onto the vibrations of a bluff body in a shear flow. A central argument in Stansby's development is that the wake of an oscillating body is in agreement with the concept of universal wake similarity. This means that a Strouhal number can be defined that is independent of the characteristic dimensions and flow separation conditions of the body. Griffin (18) recently has demonstrated that vibrating bluff bodies follow the principle of universal wake similarity and has shown in addition (19) that the principle is valid for a wide variety of structural cross-sections at Reynolds numbers from 200 to 10^7. Thus Stansby's method can be employed with some confidence to give at least a preliminary estimate of the spanwise extent over which locking-on occurs for a bluff body in a shear flow for the subcritical ($Re < 10^5$) Reynolds number range (see Section 5 of this report).

A program of experiments recently was conducted to assess the effects of shear on vortex shedding from smooth and rough cylinders at large Reynolds numbers. The results have been reported by Peltzer and Rooney (20). The experiments were conducted with a cylinder of aspect ratio L/D = 16 at Reynolds numbers in the range of 1.5 × 10^5 to 3 × 10^5 in order to assess the minimum shear (as denoted by the shear parameter $\bar{\beta}$ given above) at which the characteristic lengthwise cellular vortex shedding pattern was initiated. An incipient cellular pattern of vortex shedding was observed at the weakest shear gradient, $\bar{\beta} = 0.007$, and persisted in stronger form over the test range to shear levels given by $\bar{\beta} = 0.04$. Most of the test runs, however, were carried out at values of the shear parameter, $\bar{\beta} = 0.007$ to 0.02, which are representative of full-scale marine and atmospheric site conditions. The results obtained by Peltzer and Rooney provide a reasonably wide data base of circumferential mean pressure and vortex shedding frequencies for smooth and rough circular cylinders at subcritical, critical and supercritical Reynolds numbers.

Experiments to study the effects of a linear shear flow on the vortex shedding from circular cylinders presently are being conducted by Peterka, Cermak and Woo (21). The aspect ratios of the cylinders range from L/D = 12 to 128 over a Reynolds number range from Re = 1000 to 8000. Wake frequency spectra, base pressures and wake widths downstream from stationary cylinders have been measured for steepness parameters from $\bar{\beta}$ = 0.016 to 0.064, and similar experiments are being conducted with stationary and vibrating circular cylinders over a range of steepness parameters from $\bar{\beta}$ = 0.012 to 0.128.

The literature relating to nonuniform flow past bluff bodies is relatively sparse as compared to the corresponding uniform flow case. Most of the important papers concerned with this complex phenomenon are discussed here and in the next two sections. The major known characteristics of vortex shedding from stationary and vibrating bluff bodies in nonuniform flows, including the effects of body oscillations, are discussed there in further detail.

3. THE CHARACTERISTICS OF SHEAR FLOW PAST STATIONARY BLUFF BODIES

The basic features of shear flow past bluff bodies now are known for certain restricted conditions. These conditions are somewhat limited in that most experiments have been concerned with wind tunnel studies of vortex shedding from stationary D-shaped cylinders, rectangular bodies and, in some cases, circular cylinders. Some less basic studies of shear effects on the flow past circular cylinders have been made in water. From these experiments the following general characteristics have emerged:

(i) The vortex shedding from a D-shaped bluff body takes place in spanwise cells, with the frequency constant over each cell. The Strouhal number is constant for each cell when it is based on the body diameter and a characteristic velocity. The latter is usually the velocity measured at the body's half-span (9, 10).

(ii) The base pressure (or drag) distribution along the span of a D-shaped body in a shear flow is essentially the same as for the uniform flow case when the non-dimensionalizing velocity is the half-span value (9, 10).

(iii) The cellular vortex shedding pattern likewise is found for the case of circular and rectangular cylinders spanning a wind tunnel (11, 12, 13, 17, 20). The number of cells, however, seems to be dependent upon the aspect ratio (L/D) of the cylinder, end effects, etc. (11, 13, 17) for cylinders with $L/D < 20$. Only preliminary results are available (21) for $L/D > 20$.

(iv) The base pressure or drag force variation along a circular cylinder is dependent on the aspect ratio (L/D) of the body and is highly sensitive to end conditions (11, 12, 16, 17, 20), for $L/D < 20$. The effects of the end condition become more pronounced when the body has a free end and does not completely span the wind tunnel (12,16).

(v) When the shear flow is highly turbulent ($v'/V \sim 5\%$ or greater), a reduction in the critical Reynolds number by a factor of ten has been observed in the case of a circular cylinder (17). The effects of the linear shear flow are similar to a uniform flow of high turbulence level. The shear flow "steepness parameter" was $\bar{\beta} = 0.18$ in these experiments; this is considerably greater than the range, $\bar{\beta} = 0.01$ to 0.05, that is typical of most laboratory studies (10, 11, 13, 15). In another study of the flow around a rectangular cylinder (chord W/thickness D = 0.5) in a highly turbulent stream ($v'/V \sim 10\%$), the steepness parameter was $\bar{\beta} = 0.11$, also a relatively high value (14). These experiments once again revealed the formation of cells of constant vortex shedding frequency along the body, with the transition from cell to cell taking place over a greater length of the cylinder than for low turbulence shear flows. The peaks in the frequency spectra also were much broader than in the analogous low-turbulence shear flow.

(vi) Surface—roughened circular cylinders also exhibit the characteristic cellular vortex shedding pattern in low- and moderate-turbulence shear flows (20). This was observed for both subcritical and supercritical Reynolds numbers, with a wide range of steepness parameters, $\bar{\beta} = 0.007$ to 0.04. Any linear shear (as low as $\bar{\beta} = 0.007$) was found to trigger a cellular vortex shedding pattern over the length of the cylinder with an aspect ratio of $L/D = 16$. A general

trend toward decreasing cell length with increasing shear was found along with an increase in the average cell length with cylinder roughness.

Some typical results from the studies summarized above now are discussed. Peltzer and Rooney (20) have conducted the most complete and up-to-date study of the effects of shear on vortex shedding from circular cylinders. The Reynolds numbers for their experiments spanned the range from $Re = 1.6 \times 10^5$ to 3.6×10^5, for smooth and roughened cylinders (roughness $\delta/D = 1 \times 10^{-3}$), and steepness parameters from $\bar{\beta} = 0$ (uniform flow) to $\bar{\beta} = 0.041$. This range of parameters was sufficient to provide both subcritical, critical (or transcritical), and supercritical vortex shedding conditions. Some of the uniform flow baseline conditions for the smooth and rough cylinders are plotted in Fig. 1, along with some recent measurements by Buresti and Lanciotti (22) and by Alemdaroglu, Rebillat and Goethals (23). The three Reynolds number ranges just mentioned are noted in Fig. 1. The critical Reynolds number Re_δ of 200 to 250 is in good agreement with the value of $Re_\delta = 200$ found by Szechenyi (24). It appears that full supercritical conditions are not reached in the range of Re_δ plotted in Fig. 1, since Szechenyi found that St did not become constant again until a range of $Re_\delta = 800$ to 1000 was reached. Alemdaroglu, Rebillat and Goethals also obtained full supercritical conditions as the roughness Reynolds number approached $Re_\delta = 1000$. The supercritical Strouhal numbers measured by Szechenyi were slightly higher ($St \sim 0.26$) than those plotted in Fig. 1.

When shear was added to the incident flow the results were as shown in Fig. 2 for a typical example. The spanwise variation of the Strouhal number at this Reynolds number ($Re = 2.6 \times 10^5$) and steepness parameter ($\bar{\beta} = 0.016$) indicates a two-cell vortex shedding structure with two end plate cells. The frequency spectra and circumferential pressure coefficients plotted by Rooney and Peltzer clearly show this case to be subcritical. At the same steepness parameter, $\bar{\beta} = 0.016$, the rough cylinder exhibited supercritical shedding over the high velocity portion of its length for $Re = 2.6 \times 10^5$, while the remainder of the cylinder over the low velocity portion of the shear profile remained in the critical range.

In one of the earliest studies of shear flow past bluff bodies, Maull and Young (9, 10) conducted wind tunnel experiments to measure the vortex shedding from a D-section cylinder (chord W/thickness D = 6) with a blunt base. The cylinder had a length-to-thickness ratio of L/D = 20 and was placed in a shear flow with a steepness parameter $\bar{\beta} = 0.025$. The base pressure coefficient C_{pb_M} and the Strouhal number St_M based upon the center-line velocity V_M are shown in Fig. 3. The vortex shedding took place in four cells of constant frequency along the span of the cylinder. One cell extends from $y/D = 0$ to 6 and the second from $y/D = 7$ to 10. The third cell extends from $y/D = 10$ to 15 and the last appears at $y/D = 16$.

Frequency spectra recorded by Maull and Young showed that the cell boundary regions ($y/D = 7$, as one example) were marked by two characteristic frequencies, one from each of the adjacent cells. The variation of the base pressure in Fig. 3 shows marked changes at the cell boundaries, with noticeable variations in the C_{pb_M} versus y/D curve at $y/D = 6$ and 10. Within each vortex shedding cell the frequency of shedding was constant while the base pressure varied along the span of the cylinder. A study of flow visualization photographs by Maull and Young indicated that the cells were divided by longitudinal vortices aligned with the free-stream direction (10).

The effect of a sheared, turbulent incident flow on the vortex shedding from a circular cylinder was studied by Davies (17). The steepness parameter of the flow was $\bar{\beta} = 0.18$ and the turbulence level was about $v'/V = 5\%$. End plates were fitted to the cylinder at $\pm 3D$ from the center line of the wind tunnel. The base pressure coefficient at the mid-span location on the cylinder is plotted against the Reynolds number in Fig. 3. Also plotted in the figure for comparison are base pressure measurements that had been made in uniform smooth and turbulent flows at the National Physical Laboratory. It is clear that the onset of the critical Reynolds number is reduced in the shear flow by a factor of ten from the uniform smooth flow value of $Re = 2$ to 3×10^5. The reduction in Re_{crit} is similar to that produced by a uniform flow of the same turbulence intensity.

Additional measurements of base pressure were made by Davies along the length of the cylinder, for different mid-span Reynolds numbers. For subcritical conditions a well-defined cell structure with a predominant wake frequency and strong vortex shedding was observed. Both the base pressure coefficients based on local velocity and the mid-span value gave a clear picture of the cell boundaries. The shedding patterns became more irregular as the incident flow velocity was increased, and by Re = 10^5 any trace of a vortex shedding peak had disappeared into the turbulent background of the frequency spectrum.

Vickery and Clark (16) studied the structure of the vortex shedding from a slender, tapered circular cylinder in smooth and turbulent shear flows at subcritical Reynolds numbers between 2×10^4 and 7×10^4. The cylinder had a base diameter $D = 65$ mm (2.55 in.), a taper of 4 percent, and an aspect ratio of $L/D = 14$. A vortex shedding pattern with three cells of nearly constant frequency was observed in the smooth uniform flow, a finding which is analogous to the case of a uniform cylinder in a sheared incident flow. When the smooth flow was replaced by a shear flow with a high (4 to 10 percent) turbulence level, a continuous variation of the vortex shedding frequency was observed over the lower two-thirds of the cylinder where large changes took place ($\Delta V / V_{TIP} = 50$ percent) in the incident flow velocity. An apparent cell-like pattern with two constant-frequency cells continued to exist over the upper third of the cylinder near the free end where the incident flow velocity changed very slowly. Vickery and Clark also measured base pressure, drag and lift coefficients at close intervals along the cylinder. The base pressure coefficient based on the local velocity varied only slightly about $C_{pb} = -0.8$ in smooth flow, but in the turbulent shear flow C_{pb} varied from -0.6 near the cylinder's free end, to -0.9 at half the distance along the cylinder, and to $C_{pb} = -1.05$ near the base. Both the average drag coefficients and base pressures were substantially (25 percent) lower than typical values reported for uniform circular cylinders at the same Reynolds numbers. Based upon their experiments, Vickery and Clark developed a forced vibration aeroelastic model for predicting small displacement amplitude ($Y/D < 0.01$) vortex-excited oscillations. No account was taken of the nonlinear resonance between

the structural motion and the cross flow oscillations that is well known at larger displacement amplitudes.

Peterka, Cermak and Woo (21) are conducting experiments to study the vortex shedding from large aspect-ratio (L/D = 12 to 128), stationary and vibrating circular cylinders in a linear shear flow. Figure 5 shows the Strouhal number based on centerline velocity for the L/D = 34, $\bar{\beta}$ = 0.032 and Re = 4000. This figure confirms the two cells at the boundaries and shows a tendency toward a cellular vortex pattern over the central section of the stationary cylinder. Regions with a similar frequency can be identified over a limited distance, but it is not clear that cells with well-defined boundaries exist. When the data from Fig. 5 are presented as Strouhal numbers based on the local velocity (21), the data are grouped around Strouhal numbers of 0.2 to 0.21. The data indicates that some cellular structure occurs but that no clear cell boundaries can be identified in many regions.

Two smoke visualization photographs of the wake of the same cylinder at a Reynolds number slightly below 2000 are shown in Fig. 6. The region observed is roughly from the centerline to L = 8D below the centerline where no clear indication of a cell structure was evident from frequency measurements in the wake. The smoke was illuminated by a strobe light that was synchronized with the shedding frequency, and an exposure time long enough to cover about six or seven shedding cycles was used. The periodic structure seen in the smoke pattern along the cylinder length is a result of smoke introduction through equally spaced holes in the base of the cylinder. If a coherent cell shedding at the strobe frequency for seven or eight cycles existed during the exposure time, the result would appear as a banded system as seen in the top photograph. If a cell with a frequency different from the strobe frequency was shedding or if no shedding occurred during the exposure time, the result would look like the bottom photo. However, the photos in Fig. 6 were taken at two different times using the same strobe frequency. These results suggest that cells of finite size, but of different frequencies and extent, exist at different times in the wake (21). An inclined pattern of vortex shedding similar to that shown in the top photograph was observed by Stansby (15) for a cylinder with L/D = 16, $\bar{\beta}$ = 0.025 and Re $\approx$ 3000.

4. THE EFFECTS OF BODY OSCILLATIONS

The combined effects of velocity gradients and body oscillations are difficult to quantify on the basis of available evidence. However, the relatively sparse information that is available suggests that model and full-scale cylindrical structures will vibrate at large displacement amplitudes in both air and water even in the presence of nonuniform flow effects if the reduced damping is sufficiently small and the critical reduced velocity is exceeded (see Fig. 4 and Appendix I). Some detailed experiments reported just recently by Kwok and Melbourne (25) give strong evidence that a flexible bluff structure with a circular cross-section will vibrate resonantly at large displacement amplitudes when a turbulent boundary layer type of shear flow is incident upon the cylinder. Kwok and Melbourne measured large tip displacements of up to $\bar{Y} = 0.3$ D for reduced dampings in the range $k_s = 2$ to 12 ($\zeta_s/\mu \sim 0.5$ to 3). A typical example of their findings is given in Fig. 7.

Stansby (15) investigated the phenomenon of lock-on for the cross flow vibrations of circular cylinders in a linear shear flow and has compared the results to comparable experiments in uniform flow. From these experiments Stansby developed empirical equations to predict the bounds for lock-on in a shear flow, based upon the assumption of universal similarity of the flow in the wakes of bluff bodies (18,19). The boundaries of the cross flow lock-on regime that were measured by Stansby are shown in Fig. 8. However, these results are limited to cylinders with small length/diameter ratios (L/D = 8 to 16), relatively low Reynolds number (Re = 3000 to 10,000) and small displacement amplitudes ($\bar{Y}/D < 0.2$). These results are considered in further detail in the next section of this report.

The measured Strouhal numbers for stationary and vibrating circular cylinders in a shear flow are compared in Fig. 9. The measurements were reported by Stansby (15) for $Re_M \approx 4000$ and $\bar{\beta} = 0.025$. The stationary cylinder wake is dominated by two end cells with an irregular type of vortex shedding between these cells. This irregular region is characterized by a wide frequency spectrum which represents a range of cell shedding conditions, and the Strouhal number ranges in Fig. 9(a) define the ranges of possible constant-frequency vortex shedding cell formation. When the same cylinder was

oscillated at a forced Strouhal number of $St_{M.C.} = 0.198$, the vortex shedding over the center portion of the cylinder was dominated by a single cell from $\bar{z}/D = -1$ to $+4$ that was locked to the vibration frequency as shown in Fig. 9(b). The three unforced cells that are distributed along the cylinder show considerably more regularity in shedding frequency than do the corresponding cells on the stationary cylinder.

A recent paper and a report by Fischer, Jones and King (26,27) describe some problems that were anticipated during the installation of foundation piles for the Shell Oil production platform in the Cognac field of the Gulf of Mexico. The problems largely stemmed from the predicted vortex-excited oscillations of the piles while they were being lowered from a derrick barge into sleeves in the platform bas and while the inserted piles were being hammered into the sea bed. Maximum tip displacement amplitudes (cross flow) of 3.2 to 3.8 m (10.5 to 12.5 ft) from equilibrium were predicted for currents as low as 0.6 m/s (0.31 kt) at the platform site. These large-scale motions were expected to create difficulties while "stabbing" the piles into the sleeves, and they could also increase the risk of buckling and fatigue failures during the pile driving operations. Experiments were conducted with model piles in three laboratories, for both the pile lowering and the pile driving operations. Uniform and nonuniform (shear) flows were modelled in the experiments. For the small-scale experiments reported by Fischer, Jones and King (26,27) the shear parameter was $\bar{\beta} = 0.01$ while at the actual Cognac site $\bar{\beta} = 0.01$ at depths between 100 m (330 ft) and 250 m (820 ft).

The results from some typical model-scale experiments are plotted in Fig. 10. The tests were conducted with a 1:168 scale model of the large marine piles of diameter $D = 2.1$ m (6.9 ft). Both the full-scale and the model piles had specific gravities of 1.5. It is clear from the results in Fig. 10 that a shear flow with $\bar{\beta} = 0.01$ to 0.015 had virtually no effect on the vortex-excited displacement amplitudes in the cross flow direction. The data plotted in the figure correspond to a free-cantilever flexible beam with no tip mass at the free end. This configuration matched closely the "stabbed" pile before an underwater hammer was attached for driving it into the sea bed. The structural damping of the PVC model

in Fig. 10 was $\zeta_s = 0.063$ and for a similar stainless steel model the damping was $\zeta_s \approx 0.015$; the two flexible cylinders experienced tip displacement amplitudes of $2\bar{Y} = 3D$ and 4D, respectively. These damping and displacement amplitude values are in the range of mass and damping parameters where hydrodynamic effects are dominant (28); see Fig. A1.

It was concluded from a study of the static and dynamic stress levels within the Cognac piles during driving that the large cross flow displacement amplitudes (of the level shown in Fig. 10) would triple the stresses from a corresponding stationary 130 m (426 ft) long pile (26). The apparent steady drag coefficient on the oscillating pile was $C_D = 2.12$; this is an amplification of 230 percent from the drag coefficient $C_{DO} = 0.93$ when the pile was restrained. A fatigue life of four days was predicted for a stabbed pile (without a hammer attached) when it was exposed to a current of 0.46 m/sec (0.9 kt) in magnitude. Additional details and assumptions pertaining to the study are discussed in references 26 and 27.

A flag-type or flexible tail fairing type of wake interference device was developed to suppress the cross flow oscillations. Such a device was tested successfully on the model piles, but the particular configuration was chosen because of the nearly unidirectional currents at the Cognac platform site. Few actual problems were encountered during the field installation, but in the case of one pile typical peak-to-peak displacement amplitudes of 3 m (9.8 ft) were measured. The cause of these cross flow oscillations was attributed to alternate vortex shedding.

Experiments with flexibly-mounted cylinders in uniform and shear flows were conducted in a wind tunnel by Howell and Novak (29). When the complications of various types of turbulence and boundary layer-type shear profiles were added to the case of a low-turbulence uniform flow, Howell and Novak found that the displacement response of the cylinder was largely independent of the flow characteristics *if the structural damping was sufficiently small to cause lock-on.* Examples of four types of incident wind flow and their effect on the displacement amplitude response of a circular cylinder are shown in Fig. 11.

As the damping ratio was increased from the value ($\zeta_s = 0.01$) corresponding to the results in Fig. 11, the displacement response of the flexibly-mounted cylinders became susceptible to the characteristics of the incident flow to the cylinder. The measured displacement amplitudes compare very well with those found by other investigators, and full lock-on was observed for this cylinder with $\zeta_s = 0.01$ and $\bar{Y}/D \approx 0.5$. Fig. 12 shows a flexibly mounted circular cylinder that is placed in a deep turbulent boundary layer. The large cross flow displacement amplitude of the cylinder is plainly visible in the photograph. These findings demonstrate further that flexible cylindrical structures with small reduced damping ζ_s/μ will be susceptible to resonant vortex-excited oscillations even if the incident flow is highly nonuniform.

Kwok and Melbourne (25) also studied the cross flow response of a flexibly-mounted square cylinder. A similar variation of the displacement amplitude with structural damping as had been observed with a circular cylinder was found again for the square cylinder in the boundary layer type of incident shear flow. Other studies with square and rectangular cross-section models are discussed in the Proceedings of the Fifth International Conference on Wind Engineering, held in 1979 (30) and the Proceedings of the Fourth International Conference on Wind Effects on Buildings and Structures, held in 1975 (31).

5. METHODS FOR ESTIMATING THE BOUNDS OF FREQUENCY LOCK-ON IN A SHEAR FLOW

It is possible, based up the recent work of Stansby (15) and Griffin (18,19), to predict the spanwise extent over which the vortex shedding is locked onto the vibrations of a circular cylinder in a shear flow. The extension of the results for a rigid cylinder to the case of a slender bluff body such as a cable or other flexible bluff structure is straightforward, as recent findings have shown (32,33).

The spanwise extent Δz over which the vortex shedding is locked onto the vibrations is dependent upon the steepness parameter $\bar{\beta}$ of the shear flow, the vibration or strumming frequency and the dis-

placement amplitude of the vibration. It is reasonable to assume, in the case of a vibrating flexible structure, that the locking-on is given by the relation (15)

$$\frac{\Delta\bar{z}}{D} = 3.4\left(\frac{\bar{Y}}{D}\right)\bar{\beta}^{-1},\ \bar{\beta} > 0. \tag{2}$$

The shear flow steepness parameter again is given by

$$\bar{\beta} = \frac{D}{V_{REF}}\frac{dV}{d\bar{z}},\ V_{REF} = V_M, \tag{1}$$

and some typical results for Δz are listed in Table 1 for representative values of the cross flow displacement amplitude and the steepness parameter. Calculations in the table are limited to $\bar{Y}/D < 0.5$ since the equation has been verified for small displacement amplitudes. A practical upper limit for $\bar{Y}$ is about 1 to 1.5 D, as is well known (34,35); see Fig. A1. The steepness parameters in Table 1 are representative of the ranges studied by Stansby (15), $\bar{\beta} = 0.025$ and 0.05; Davies (17), $\bar{\beta} = 0.18$; and Rooney and Peltzer (20), $\bar{\beta} = 0.007$ to 0.04. It can be seen from the results in the table that the spanwise extent of the resonant, vortex-excited oscillations can extend over many multiples of a diameter, $\Delta z =$ 50 to 80 D, so that spanwise extents that approach the half-wavelength of a marine cable or the aspect ratios of other long, flexible structures are possible.

Table 1
Estimation of the Spanwise Extent of
Resonant, Vortex Excited Oscillations for
a Circular Cylinder in a Shear Flow

SPANWISE EXTENT, $\Delta\bar{z}/D$		SHEAR FLOW STEEPNESS PARAMETER, $\bar{\beta}$			
		0.02	0.05	0.10	0.20
	0.2	34	13.6	6.8	3.4
MAXIMUM VORTEX-EXCITED	0.3	51	20.4	10.2	5.1
DISPLACEMENT, $\bar{Y}/D$	0.4	68	27.2	13.6	6.8
	0.5	85	34	17	8.5

Note: The spanwise distance $\Delta\bar{z}$ and the displacement amplitude $\bar{Y}$ are expressed in multiples of the cylinder diameter D.

King (27) found in his model tests with slender, cantilevered cylinders in water that large-amplitude, resonant cross flow oscillations ($\bar{Y}$ = 1 to 1.5 D) were readily excited in the first bending mode when the aspect ratio L/D = 52. The vortex shedding was locked onto the vibration over much of the length of the structure which was placed in a shear flow with a steepness parameter of $\bar{\beta}$ = 0.01 to 0.015. Kwok and Melbourne (25) and Howell and Novak (29) found that lock-on was readily obtained in boundary layer shear flows over lengths of L = 9 to 10 D with flexibly-mounted circular cylinders that were excited to cross flow displacement amplitudes of $\bar{Y}$ = 0.15 to 0.25 D (see Figs. 7 and 11).

6. CONCLUDING REMARKS

6.1 Summary. The flow about stationary and vibrating bluff bodies in a shear flow has undergone increasingly intensive study over the past ten years. Bluff cylinders both circular and non-circular in cross-section have been utilized in both wind tunnel and water channel experiments conducted to investigate the susceptibility of structures to vortex excited oscillations. All of the experiments conducted to date with stationary cylinders have demonstrated that a cellular pattern of vortex shedding exists along the span of the body. Over each cell the vortex shedding frequency is constant, and the constant values of the Strouhal number and the base pressure coefficient are obtained when a characteristic velocity scale (usually, the mid-span value) is employed. A most important finding from several of the studies conducted thus far is that lightly damped structures both circular and non-circular (square and D-section) in shape undergo large amplitude cross flow oscillations in linear and boundary layer type shear flows of air and of water.

Some experiments also have been conducted to investigate the effects of turbulence on the response of cylinders in a shear flow. In the case of a linear shear flow with high turbulence level it was observed that the critical Reynolds number for a stationary circular cylinder was reduced by a factor of ten as had been found for the related case of an incident uniform flow. The vortex-excited cross flow response of a circular cylinder was found to be insensitive to the level of incident turbulence when the

damping of the structure was small enough to cause lock-on between the vortex shedding and vibration frequencies.

6.2 *Recommendations* Most of the studies conducted thus far have been limited to cylinders with small aspect ratios of length/diameter less than $L/D = 15$ to 20. The cellular structure of the vortex shedding is influenced strongly by the end conditions for cylinders with these relatively small values of L/D and so it is important to conduct experiments with cylinders of sufficient length to minimize the effects of the end boundaries. The results obtained from experiments such as these will be of particular importance in the design of long, flexible marine structures and cable arrays.

It is important also to investigate further the effects of incident shear on the cross flow response of lightly-damped structures in air and in water. The experiments conducted thus far have demonstrated that cylindrical structures undergo large-amplitude unsteady motions in shear flows when the critical incident flow velocity is exceeded and the damping is sufficiently small. However, more definitive bounds for and details of this fluid-structure interaction are required for applications in both wind engineering design of buildings and structures and ocean engineering design of structures and cable systems.

This study was conducted at the Naval Research Laboratory as part of a research program in marine cable dynamics funded by the Civil Engineering Laboratory, Naval Construction Battalion Center.

7. REFERENCES

1. E. Naudascher, (ed.), *Flow-Induced Structural Vibrations*, Springer: Berlin (1974).

2. E. Naudascher and D. Rockwell (eds.), *Symposium on Practical Experiences with Flow-Induced Vibrations (Preprints)*, Karlsruhe, German (September 1979).

3. W.J. McCroskey "Some Current Research in Unsteady Fluid Dynamics—A Freeman Scholar Lecture," Transactions of ASME, Journal of Fluids Engineering, Vol. 99, 8-39 (1977).

4. T. Sarpkaya, "Vortex-Induced Oscillations—A Selective Review", Transactions of ASME, Journal of Applied Mechanics, Vol. 46, 241-258 (1979).

5. S.E. Ramberg "The Influence of Yaw Angle upon the Vortex Wakes of Stationary and Vibrating Cylinders" NRL Memorandum Report 3822 (August 1978).

6. F.D. Masch and W.L. Moore "Drag Forces in Velocity Gradient Flow," Proceedings of the ASCE, Journal of the Hydraulics Division, Vol. 86, No. Hy 7, 1-11 (1960).

7. M.R. Starr "The Characteristics of Shear Flows Past a Circular Cylinder," Ph.D. Thesis, University of Bristol: Bristol, U.K. (1966).

8. T.L. Shaw and M.R. Starr "Shear Flows Past a Circular Cylinder," Proceedings of the ASCE, Journal of the Hydraulics Division, Vol. 98, No. Hy 3, 461-473 (1972).

9. D.J. Maull and R.A. Young "Vortex Shedding From a Bluff Body in a Shear Flow," in *Flow-Induced Structural Vibrations*, E. Naudascher ed., 717-729 (1974).

10. D.J. Maull and R.A. Young "Vortex Shedding From Bluff Bodies in a Shear Flow," Journal of Fluid Mechanics, Vol. 60, 401-409 (1973).

11. W.A. Mair and P.K. Stansby "Vortex Wakes of Bluff Cylinders in a Shear Flow," SIAM Journal of Applied Mathematics, Vol. 28, 519-540 (1975).

12. F. Etzold and H. Fiedler "The Near-Wake Structure of a Cantilevered Cylinder in a Cross-Flow," Zeitschrift fur Flugwissenshaften, Vol. 24, 77-82 (1976).

13. C. Fiscina "An Investigation Into the Effects of Shear on the Flow Past Bluff Bodies," M.S. Thesis, University of Notre Dame: Notre Dame, Indiana (May 1977).

14. C. Fiscina, "An Experimental Investigation of the Flow Field Around a Bluff Body in a Highly Turbulent Shear Flow," Ph. D. Dissertation, University of Notre Dame: Notre Dame, Indiana (May 1979).

15. P.K. Stansby "The Locking-on of Vortex Shedding Due to the Cross-Stream Vibration of Circular Cylinders in Uniform and Shear Flows," Journal of Fluid Mechanics, Vol. 74, 641-667 (1976).

16. B.J. Vickery and A.W. Clark, "Lift or Across-Wind Response of Tapered Stacks," Proceedings of ASCE, Journal of the Structural Division, Vol. 98, No. ST1, 1-20 (1972).

17. M.E. Davies "The Effects of Turbulent Shear Flow on the Critical Reynolds Number of a Circular Cylinder," National Physical Laboratory (U.K.) NRL Report Mar Sci R 151 (January 1976).

18. O.M. Griffin, "A universal Strouhal number for the 'locking-on' of vortex shedding to the vibrations of bluff cylinders," Journal of Fluid Mechanics, Vol. 85, 591-606 (1978).

19. O.M. Griffin "Universal similarity in the wakes of stationary and vibrating bluff bodies," Transactions of ASME, Journal of Fluids Engineering, Vol. 103, to appear (March 1981).

20. R.D. Peltzer and D.M. Rooney, "Effect of Upstream Shear and Surface Roughness on the Vortex Shedding Patterns and Pressure Distributions Around a Circular Cylinder in Transitional Re

Flows," Virginia Polytechnic Institute and State University Report No. VIP-Aero-110 (April 1980).

21. J.A. Peterka, J.E. Cermak and H.G.C. Woo, "Experiments on the Behavior of Cables in a Linear Shear Flow" Fluid Mechanics and Wing Engineering Program, Colorado State University, Progress Report on CONTRACT No. N68305-78-C-0055 for the Civil Engineering Laboratory, Naval Construction Battalion Center (May 1980).

22. G. Buresti and A. Lanciotti, "Vortex Shedding From Smooth and Roughened Circular Cylinders in Cross Flow Near a Plane Surface," Aeronautical Quarterly, Vol. 28, 305-321 (February 1979).

23. N. Alemdaroglu, J.C. Rebillat and R. Goethals, " A Sound Analysis Coherence Function Method Applied to Circular Cylinder Flows," Journal of Sound and Vibration, Vol. 69, 427-440 (1980).

24. E. Szechenyi, "Supercritical Reynolds number simulation for two-dimensional flow over circular cylinders," Journal of Fluid Mechanics, Vol. 70, 529-542 (1975).

25. K.C.S. Kwok and W.H. Melbourne, "Cross-Wind Response of Structures Due to Displacement Dependent Lock-in Excitation," in *Proc. Fifth Int. Conf. on Wind Engrg. (Preprints)*, Vol. II, Fort Collins, Co., VI-4 (July 1979).

26. F.J. Fischer, W.T. Jones and R. King, "Current-Induced Oscillation of Cognac Piles During Installation-Prediction and Measurements," in *Proc. Symp. Practical Experiences with Flow-Induced Vibrations* (Preprints), Karlsruhe, Vol. 1, 216-228 (September 1979).

27. R. King, "Model Tests of Vortex Induced Motion of Cable Suspended and Cantilevered Piles for the Cognac Platform," BHRA Fluid Engineering Report RR 1453 (January 1978).

28. O.M. Griffin, "OTEC Cold Water Pipe Design for Problems Caused by Vortex-Excited Oscillations," Naval Research Laboratory Memorandum Report 4157 (March 1980).

29. J.F. Howell and M. Novak, "Vortex Shedding from Circular Cylinders in Turbulent Flow," in *Proc. Fifth Int. Conf. on Wind Engrg.* (Preprints), Vol. I, Fort Collins, Co, Paper V-11 (July 1979); see also J.F. Howell, "Soil-Structure Interaction Under Wind Loading," Ph.D. Thesis, University of Western Ontario: London, Ontario (April 1978).

30. J. Cermak (ed.), *Proceedings of the Fifth International Conference on Wind Engineering* (Preprints), Colorado State University: Fort Collins, Colorado (July 1979).

31. K.J. Eaton (ed.), *Proceedings of the Fourth International Conference on Wind Effects on Buildings and Structures,* Cambridge University Press: Cambridge, UK (1976).

32. O.M. Griffin, R.A. Skop and S.E. Ramberg, " The Resonant, Vortex-Excited Vibrations of Structures and Cable Systems," Offshore Technology Conference Preprint 2319 (1975).

33. R.A. Skop and O.M. Griffin, "On a Theory for the Vortex-Excited Oscillations of Flexible Cylindrical Structures," Journal of Sound and Vibration, Vol. 41, 263-274 (1975).

34. O.M. Griffin, "Vortex-Excited Cross Flow Vibrations of a Single Cylindrical Tube," in *Flow-Induced Vibrations,* S.S. Chen and M.D. Bernstein (eds.), ASME: New York, 1-10 (June 1979); see also Transactions of ASME, Journal of Pressure Vessel Technology, Vol. 102, No. 2, 158-166 (1980).

35. O.M. Griffin, J.A. Pattison, R.A. Skop, S.E. Ramberg and D.J. Meggitt, "Vortex-Excited Vibrations of Marine Cables," Proceedings of the ASCE, Journal of the Waterways, Port, Coastal and Ocean Division, Vol. 106, No. WW2, 183-204 (1980).

36. R.B. Dean, R.W. Milligan and L.R. Wootton, "An Experimental Study of Flow-Induced Vibration" E.E.C. Report 4, Atkins REsearch and Development Ltd.: Epsom, U.K. (1977).

37. E. Simiu and R.A. Scanlan, *Wind Effects on Buildings and Structures: An Introduction to Wind Engineering*, Wiley-Interscience: New York (1978).

8. APPENDICES

1. Methods for Estimating the Susceptibility of Bluff Bodies to Cross Flow Vortex-Excited Oscillations.

General procedures. Design procedures and prediction methods for analyzing the vortex-excited oscillations of structures have been developed only since the mid 1970's. Previously a reliable experimental data base and accurate characterization of the phenomenon were relatively unavailable, and it has been only since marine construction has moved into deeper water and more harsh operating environments that the need for sophisticated design procedures has arisen. The need to design slender, flexible structures against problems due to vortex shedding in the atmospheric environment also has spurred renewed efforts to develop new wind engineering design procedures. It should be emphasized, however, that reliable data are available only at subcritical Reynolds numbers. The design procedures that are generally available have been discussed recently in a related NRL report (28).

All of the methods developed thus far are in common agreement and point out that the following parameters determine whether large-amplitude, vortex-excited oscillations will occur:

- The *logarithmic decrement* of *structural* damping, δ
- The reduced velocity, $V/f_n D$;
- The mass ratio, $m_e/\rho D^2$.

Here m_e is the *effective mass* of the structure which is defined as

$$m_e = \frac{\int_0^L m(x) y^2(x)\, dx}{\int_0^h y^2(x)\, dx} \tag{A.1}$$

where $m(x)$ is the cylinder mass per unit length including internal water or other fluid and the added mass, joints, sections of different material, etc.;

$y(x)$ is the modal shape of the structure along its length;

L is the overall length of the structure, measured from its termination;

h is the water depth.

It should be noted here that many of these methods were developed originally for structural members that pierced the water surface, hence the length L was greater than the depth h. The effective mass m_e then defines an equivalent structure whose vibrational kinetic energy is equal to that of the real structure.

As described in reference 28, the mass parameter and the structural damping can be combined as

$$k_s = \frac{2m_e\delta}{\rho D^2} \text{ or } \frac{\zeta_s}{\mu} = 2\pi St^2 k_s, \tag{A.2}$$

which in both forms are called the reduced damping. The reduced damping k_s is the ratio of the actual damping *force* (per unit length) and $\rho f_n D^2$, which can be viewed as an inertial force. Available results also suggest criteria for determining the critical incident flow velocities for the onset of vortex-excited motions. These critical velocities are

$$V_{crit} = (f_n D)\, V_{r,crit}, \tag{A.3}$$

where $V_{r,crit} = 1.2$ for in line oscillations and $V_{r,crit} = 3.5$ for cross flow oscillations at Reynolds numbers greater than about 5×10^5. For Reynolds numbers below 10^5, $V_{r,crit} = 5$.

It was noted above that the peak cross flow displacement amplitude is a function primarily of a response or reduced damping parameter when the damping is small and $\zeta_s = \delta/2\pi$. The importance of the reduced damping follows directly from resonant force and energy balances on the vibrating structure. Moreover, the relation between Y_{MAX} ($Y = \bar{Y}/D$) and k_s or ζ_s/μ holds equally well for flexible cylindrical structures with normal mode shapes given by $\psi_i(z)$, for the i th mode. If the cross flow displacement (from equilibrium) of a flexible structure is written as (28)

$$y_i = Y\, \psi_i(z) \sin \omega t$$

at each spanwise location z, then the peak displacement is scaled by the factor

$$Y_{EFF,MAX} = YI_i^{1/2} / |\psi_i(z)|_{MAX} = Y_i/\gamma_i \tag{A.4}$$

In this equation

$$I_i = \frac{\int_0^L \psi_i^4(z)\, dz}{\int_0^L \psi_i^2(z)\, dz}$$

and

$$\gamma_i = \frac{|\psi_i(z)|_{MAX}}{I_i^{1/2}}$$

which are derived from considerations based on several related versions of the so-called "wake oscillator" formulation for predicting vortex-excited oscillations. Typical values of γ_i, ψ_i and I_i are tabulated in reference 28.

An increase in the reduced damping results in smaller amplitudes of oscillation and at large enough values of ζ_s/μ or k_s the vibratory motion becomes negligible. Reference to Fig. A1 suggests that oscillations are effectively suppressed at $\zeta_s/\mu > 4$ (or $k_s > 16$). Cylindrical structures in water fall well toward the left-hand portion of the figure. The measurements of in line oscillations in water have shown that vortex-excited motions in that direction are effectively negligible for $k_s > 1.2$. The results obtained by Dean, Milligan and Wootton (36), King (27) and others shown in Fig. A1 indicate that the reduced damping can increase from $\zeta_s/\mu = 0.01$ to 0.5 (a factor of *fifty*) and the peak-to-peak displacement amplitude is decreased only from 2 or 3 diameters to 1 diameter (a nominal factor of only *two or three*). At the small mass ratios and structural damping ratios that are typical of light, flexible structures in water, the hydrodynamic forces predominate and it is difficult to reduce or suppress the oscillations by changing the mass and damping of the structure.

Table A1. Vortex-excited cross flow displacement amplitude response of cylindrical structures.	
Legend for Data Points in Fig. A1	
Type of cross-section and mounting: medium	Symbol
Various investigators, from Griffin (34):	
Spring-mounted rigid cylinder; air	* ○ ⊣ ◉ ◐
Spring-mounted rigid cylinder; water	♦
Cantilevered flexible circular cylinder; air	⅄
Cantilevered flexible circular cylinder; water	× ▽ ⊕
Pivoted rigid circular rod; air	□ ▲
Pivoted rigid circular rod; water	●
From Dean, Milligan and Wootton (36):	
Spring-mounted rigid cylinder; water	◩
Flexible circular cylinder, $L/D = 240$; water	◪
From King (27):	
Cantilevered flexible circular cylinder, $L/D = 52$ (PVC); water	◕
Cantilevered flexible circular cylinder, $L/D = 52$ (Stainless steel); water	◐

Step-by-step procedures for determining the deflection that result from vortex-excited oscillations have been developed by several groups, and these procedures are summarized in reference 28. The steps to be taken generally should follow the sequence:

- Compute/measure vibration properties of the structure (natural frequencies or periods, normal modes, modal scaling factors, etc.)

- Compute Strouhal frequencies and test for critical velocities, $V_{r,crit}$ (in line and cross flow), based upon the incident flow environment.

- Test for reduced damping, k_s, based upon the structural damping and mass characteristics of the structure.

If the structure is susceptible to vortex-excited oscillations, then

- Determine vortex-excited unsteady displacement amplitudes and corresponding steady-state deflections based upon the steady drag amplification that accompanies the oscillations.

- Determine new stress distributions based upon the new steady-state deflection and the superimposed forced mode shape caused by the unsteady forces, displacements and accelerations due to vortex shedding.

- Assess the severity of the amplified stress levels relative to fatigue life, critical stresses, etc.

These general procedures are discussed in detail in reference 28 where several practical design problems also are given as examples. Kwok and Melbourne (25) discuss applications to wind engineering design of structures from an empirical viewpoint, and Simiu and Scanlan (37) discuss applications of the wake-oscillator type of approach to applications in wind engineering.

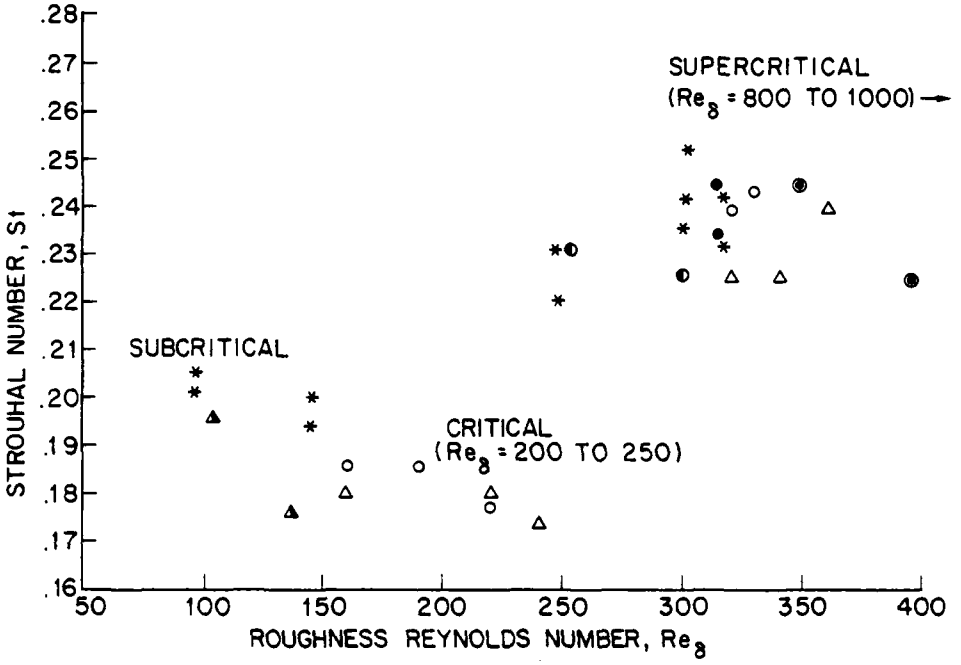

Figure 1. Strouhal number $St = f_s D/V$ plotted against the roughness Reynolds number $Re_\delta = V\delta/\nu$. Here δ is the cylinder surface roughness. Legend for data points:

Peltzer and Rooney (20):
- ○ Rough ($\delta/D = 10^{-3}$)
- △ Rough, low turbulence = .03%

Buresti and Lanciotti (22):
- • Rough ($\delta/D = 10^{-3}$)
- ● Rough ($\delta/D = 3.5 \times 10^{-3}$)

Alemdaroglu, Rebillat and Goethals (23):
- ▲ Rough ($\delta/D = 10^{-3}$)
- ◐ Rough ($\delta/D = 5 \times 10^{-3}$)
- ◉ Rough ($\delta/D = 3.4 \times 10^{-3}$)

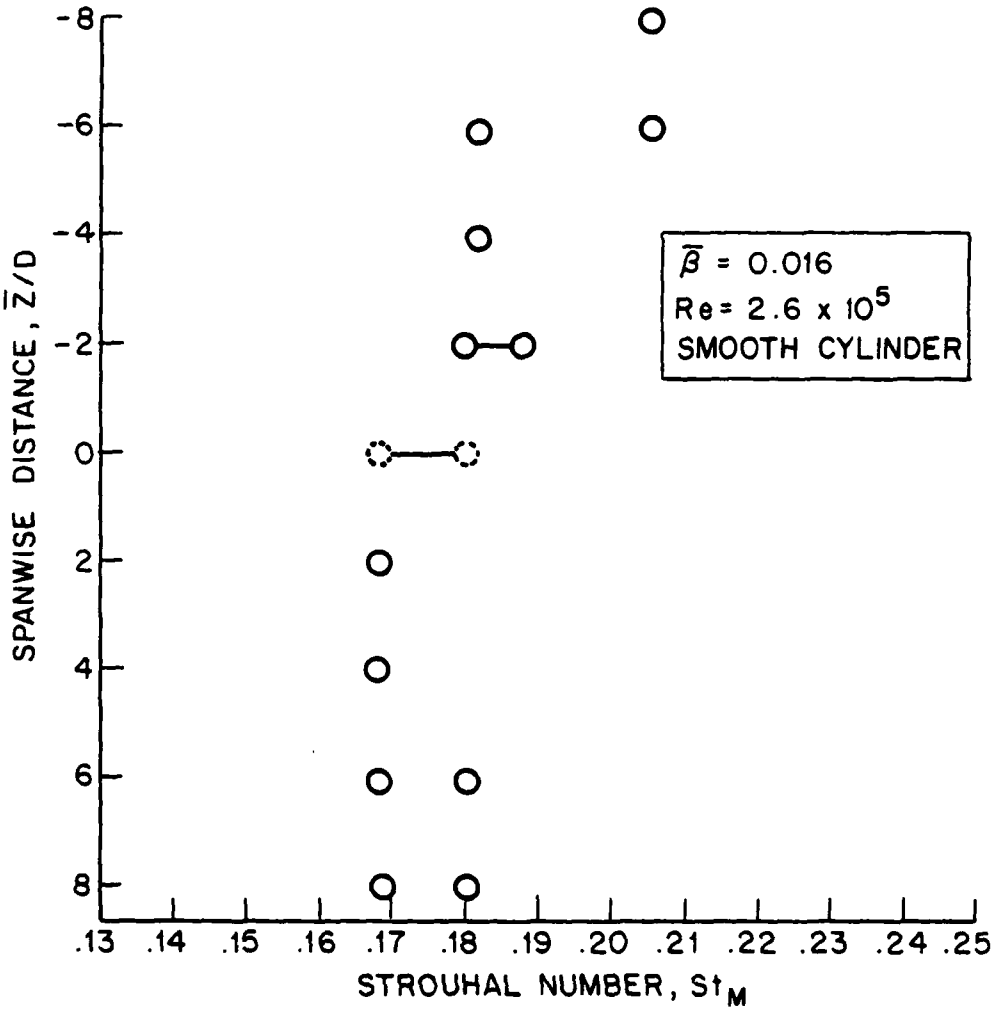

Figure 2. Strouhal number St_M (based upon the center line velocity V_M) plotted against spanwise distance along a circular cylinder in a linear shear flow; from Peltzer and Rooney (20). Reynolds number $Re_M = 2.6 \times 10^5$; shear flow steepness parameter $\bar{\beta} = 0.016$.

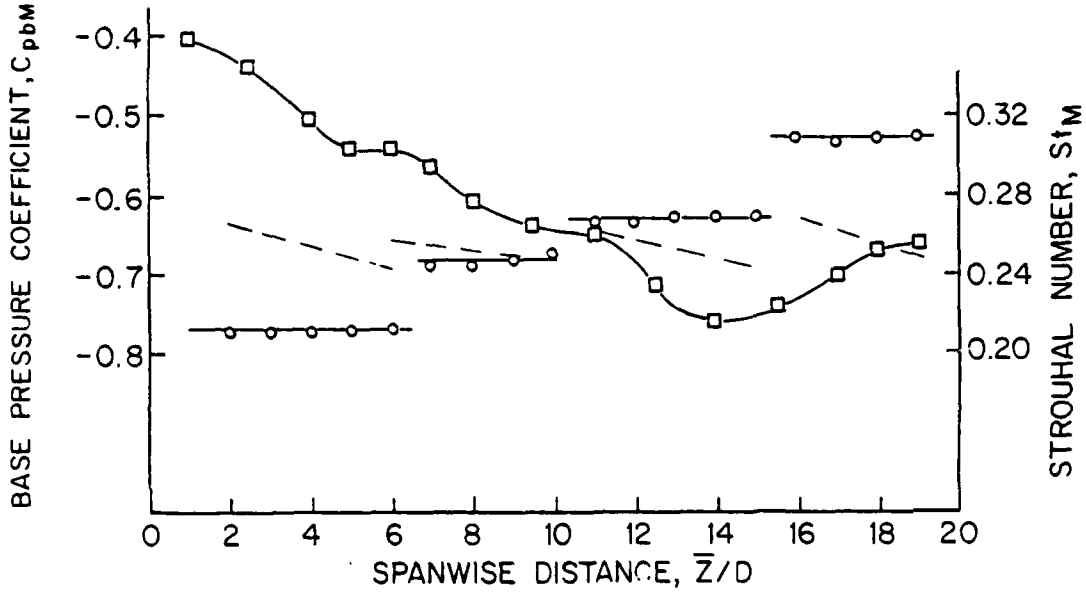

Figure 3. Base pressure coefficient C_{pbM} and Strouhal number St_M (based upon the center line velocity V_M) plotted against the spanwise distance along a D-section cylinder in a linear shear flow; from Maull and Young (10). Reprinted by permission of the Cambridge University Press. Reynolds number $Re_M = 2.8 \times 10^4$; shear flow steepness parameter $\bar{\beta} = 0.025$; cylinder chord/thickness ratio $W/D = 6$.

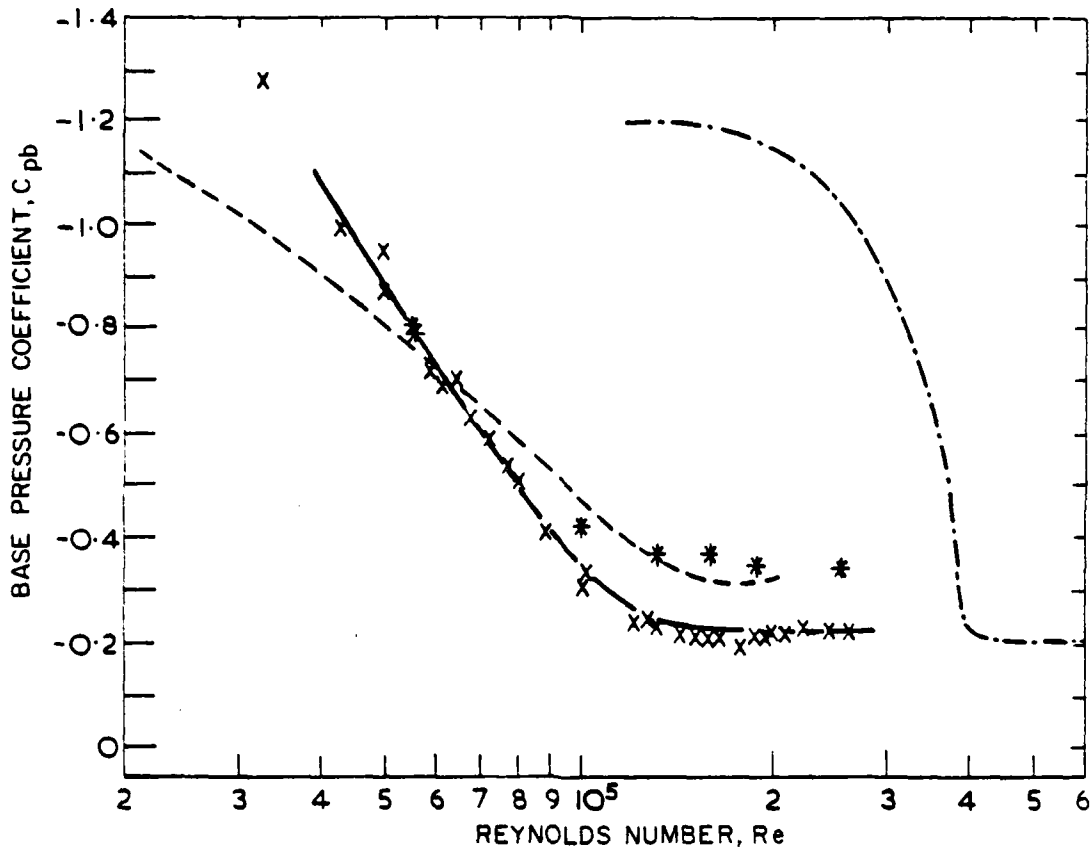

Figure 4. Base pressure coefficient C_{pb} at the center line plotted against the Reynolds number Re_M for a circular cylinder in a shear flow; from Davies (17). Legend for data:

× Center-line value, $C_{pb,M}$ ($\bar{\beta} = 0.18$)
· — · — Uniform smooth flow
----- Uniform turbulent flow (Bearman 1968)
* Average value ($\bar{\beta} = 0.18$)

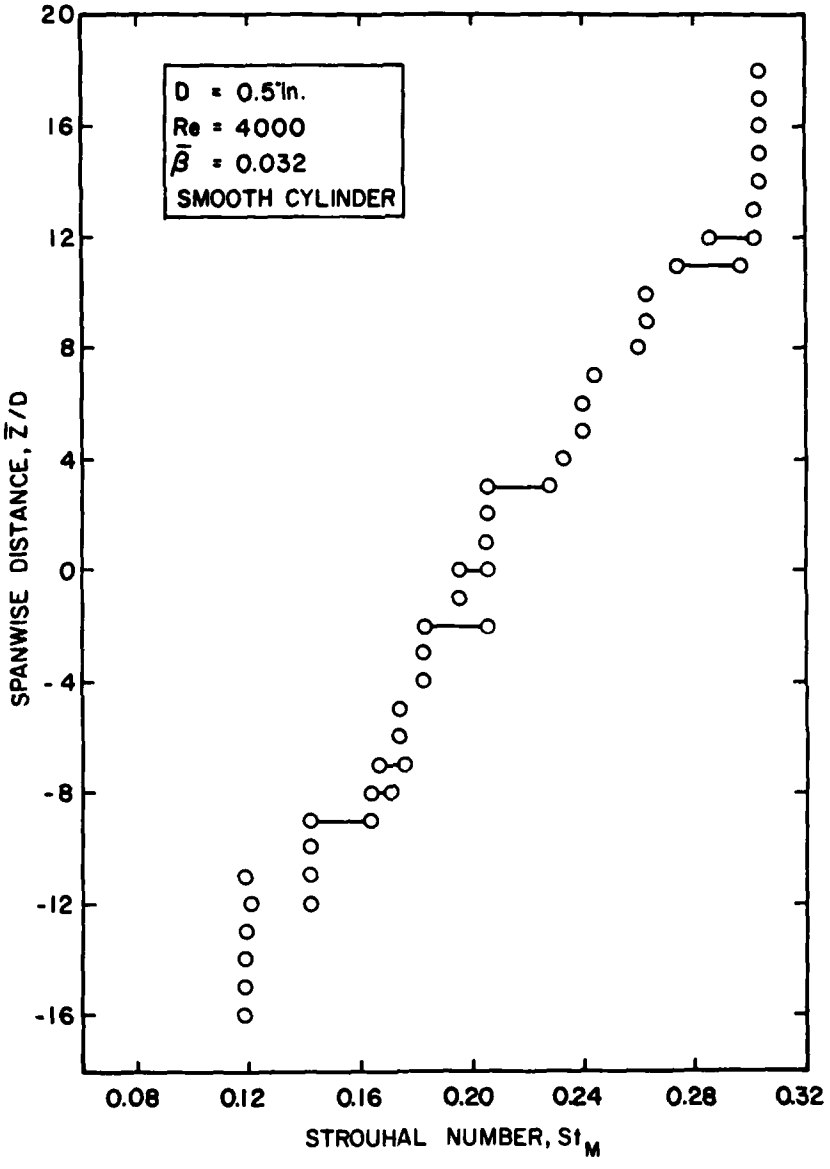

Figure 5. Strouhal number St_M (based upon the center line velocity V_M) plotted against the spanwise distance along a circular cylinder in a linear shear flow; from Peterka, Cermak and Woo (21). Reynolds number $Re_M = 4000$, shear flow steepness parameter $\bar{\beta} = 0.032$.

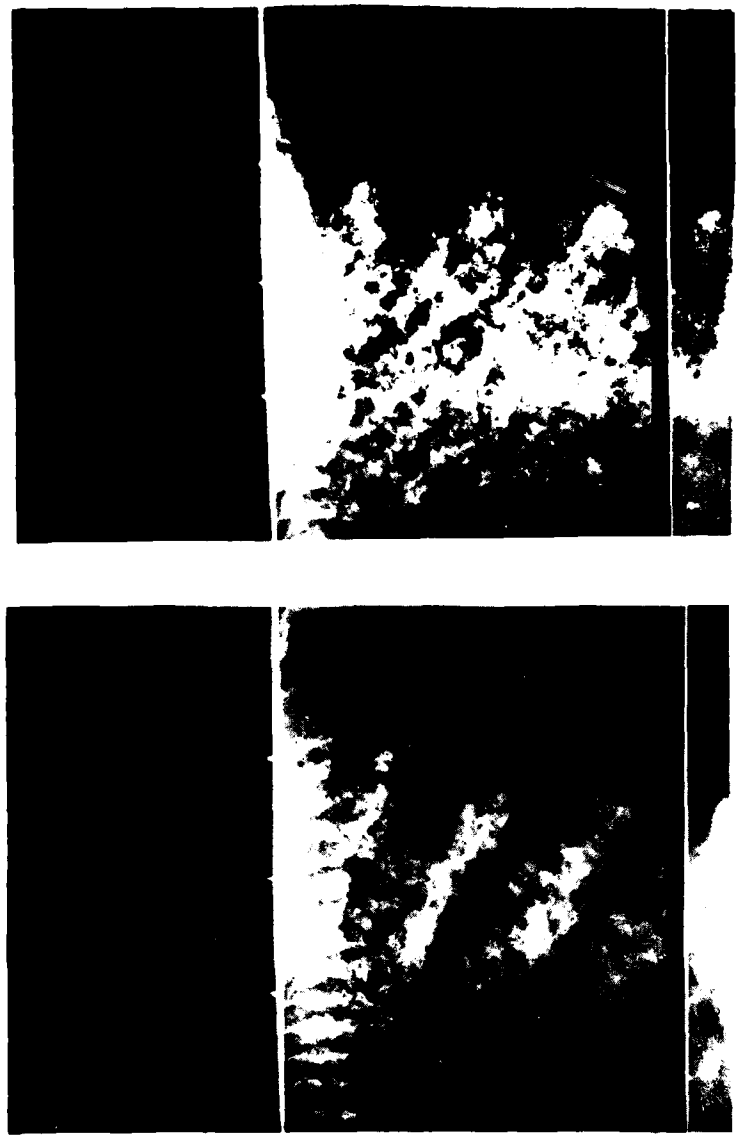

Figure 6. Long exposure photographs of vortex shedding from a circular cylinder in a linear shear flow; from Peterka, Cermak and Woo (21). Reynolds number $Re_M = 2000$; shear flow steepness parameter $\tilde{\beta} = 0.032$; cylinder aspect ratio $L/D = 20$. The photographs were provided by Dr. Jon Peterka, Colorado State University.

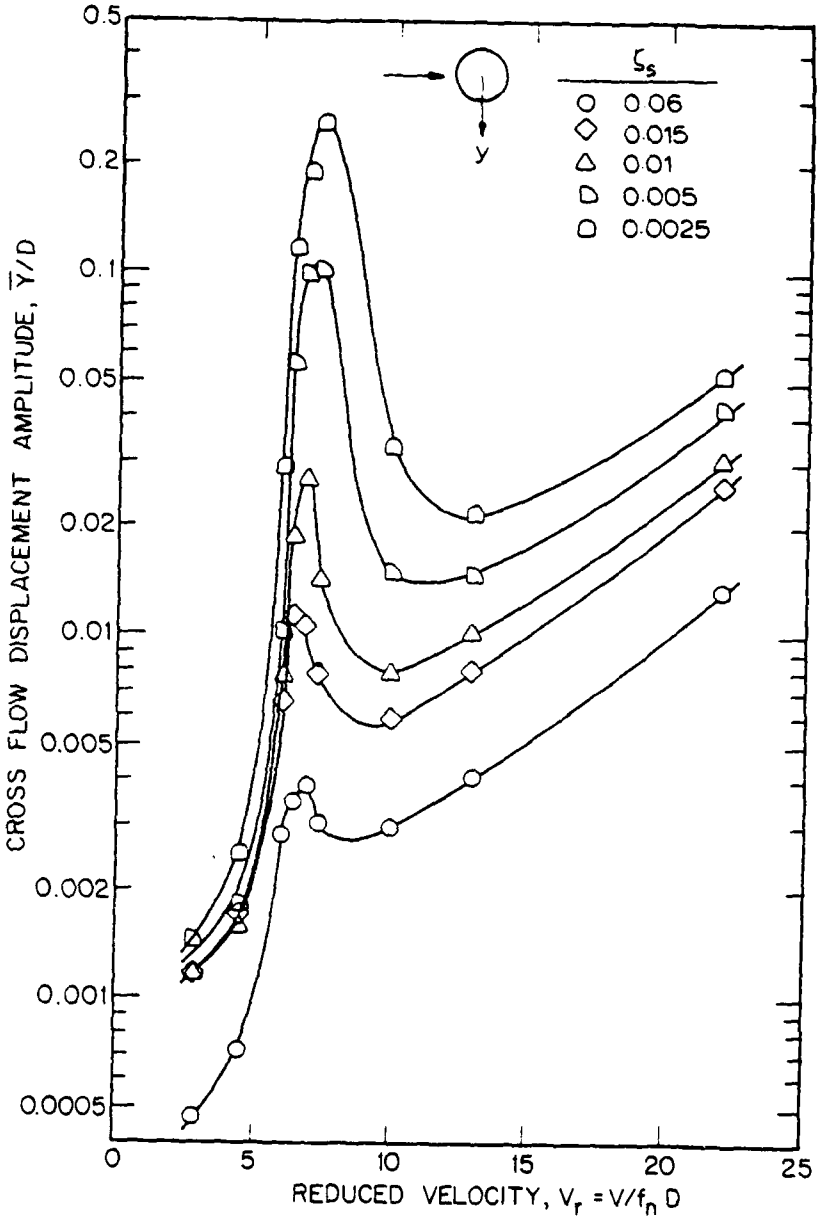

Figure 7. Peak cross flow displacement response $\bar{Y}/D$ (standard deviation of $\bar{Y}$) plotted against reduced velocity $V_r = V/f_n D$ for a model circular cylinder in a turbulent boundary layer; from Kwok and Melbourne (25). The structural damping ratio ζ_s of the rigid pivoted model was varied as shown on the figure. The characteristic flow velocity V was measured at the tip of the cylinder, of aspect ratio $L/D = 9$. The figure was provided by Dr. K.C.S. Kwok, University of Sydney, Australia.

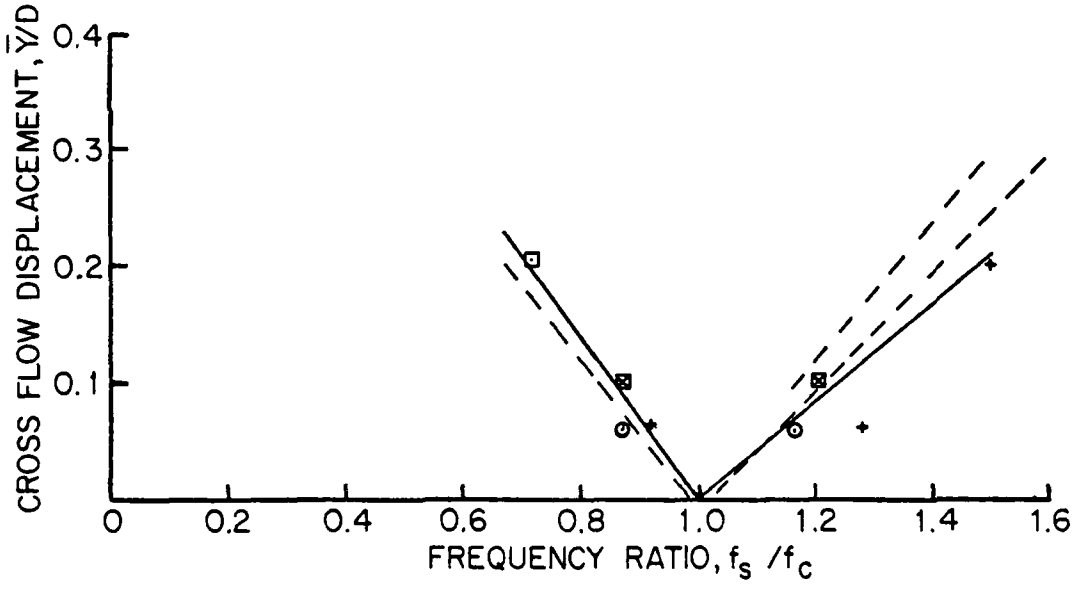

Figure 8. Boundaries of the cross flow lock-on regime in a shear flow, denoted by the displacement amplitude $\bar{Y}/D$ on the vertical scale, plotted against the ratio f_s/f_c of the Strouhal and vibration frequencies; from Stansby (15). Reprinted by permission of the Cambridge University Press. Legend for data points:

⊐ $St_{M,c} = f_c D/V_M = 0.168$, $L/D = 9$, $Re_M = 9100$;

⊃ $St_{M,c} = 0.198$

\+ $St_{M,c} = 0.155$ $L/D = 16$, $Re_M = 3700$;

⊐ $St_{M,c} = 0.174$

----- Uniform flow (15).

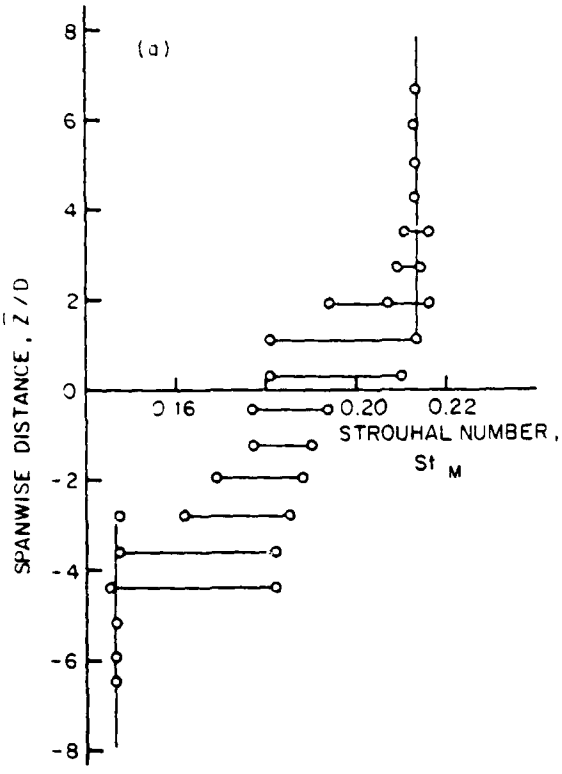

(a) Stationary cylinder. Reynolds number $Re_{sf} \approx 4000$, shear flow steepness parameter $\beta = 0.025$, cylinder aspect ratio $L/D = 16$.

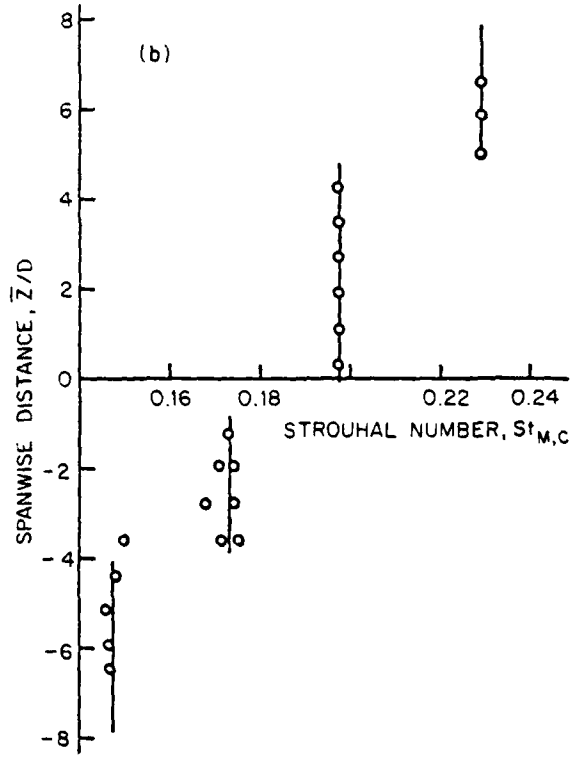

(b) Vibrating cylinder. Same conditions as Figure 9(a) except that the forced Strouhal number of the cross flow oscillation is $St_{vf,c} = 0.198$, displacement amplitude $\bar{Y}/D = 0.06$.

Figure 9. Strouhal number St_{sf} plotted against the spanwise distance along stationary and vibrating cylinders; from Stansby (15). Reprinted by Permission of the Cambridge University Press.

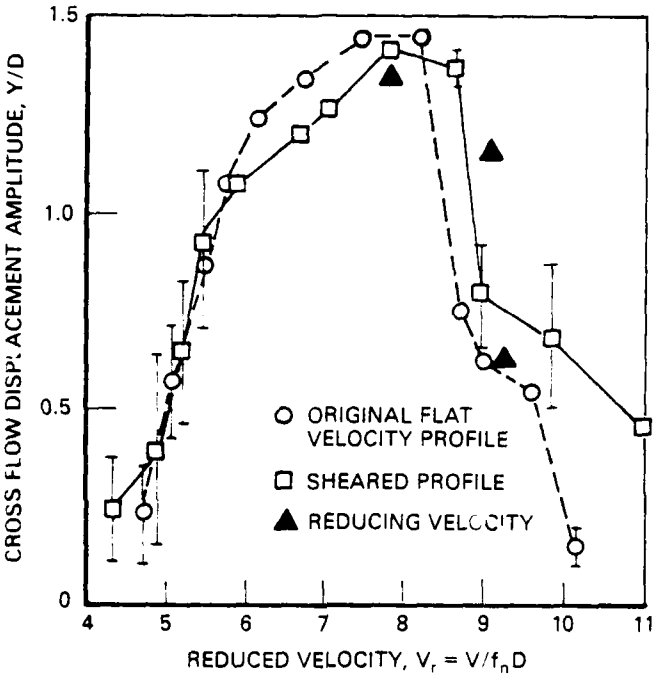

Figure 10. Measured peak cross flow displacement amplitude $\bar{Y}/D$ plotted as a function of the reduced velocity V_r. A slender, fully submerged and cantilevered circular cylinder was employed as the model (L/D = 52. D = 12.7 mm (0.5 in)) for experiments conducted in uniform ($\bar{\beta}$ = 0) and shear ($\bar{\beta}$ = 0.01 to 0.015) flows of water. The cylinder was a 1:168 scale model of a full-scale marine pile with the same specific gravity (SG = 1.5), from experiments reported by Fischer, Jones and King (26) and King (27). In the case of the shear flow V is the maximum value in the nonuniform incident velocity profile. The figure was provided by Dr. Warren Jones of the Shell Development Company.

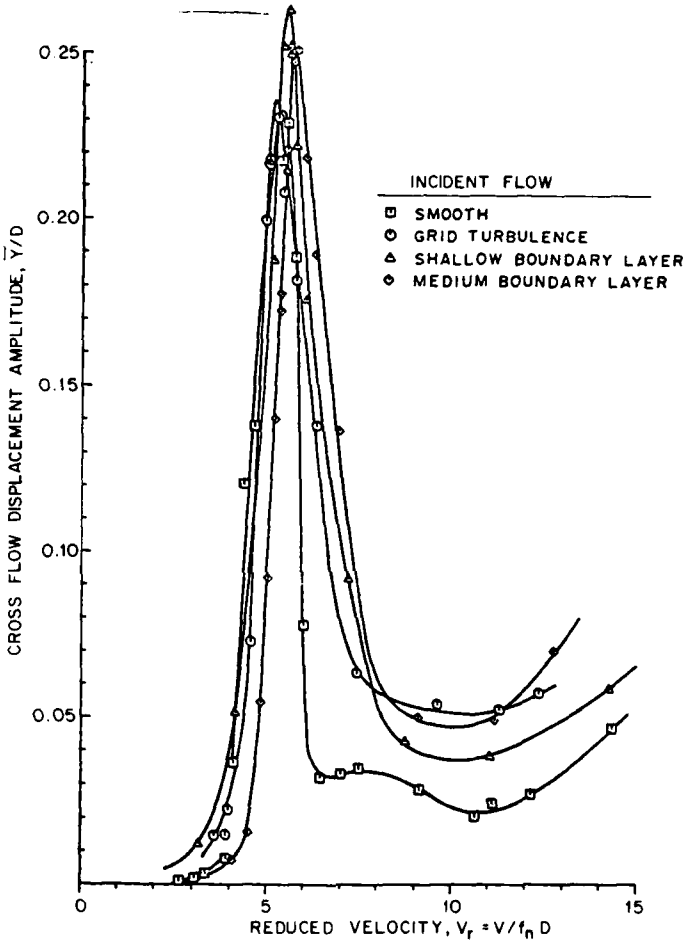

Figure 11. Peak cross flow displacement amplitude $\overline{Y}/D$ (root-mean-square of $\overline{Y}$) plotted against reduced velocity V_r for a flexibly-mounted circular cylinder in uniform and sheared incident flows; from Howell and Novak (29). Structural damping ratio ζ_s = 0.01; aspect ratio L/D = 10. The various types of incident wind flows are given by the legend. The figure was provided by Dr. John F. Howell, University of Bath, England.

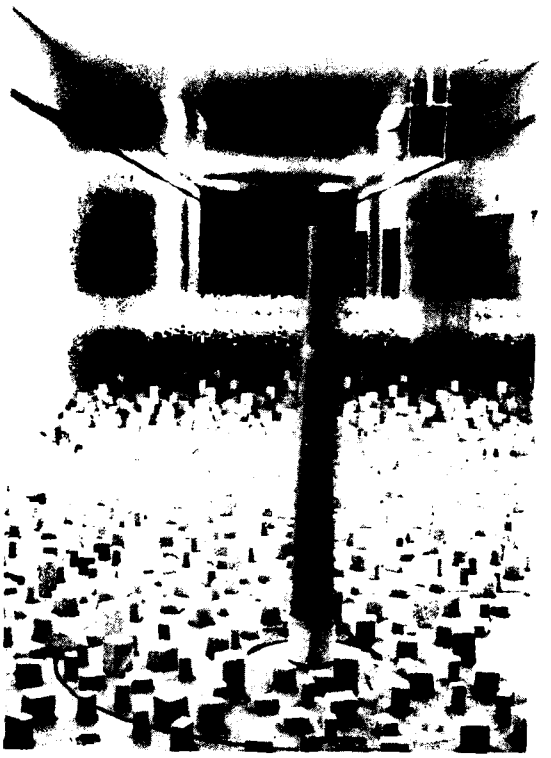

Figure 12. Cross flow oscillation of a flexibly-mounted circular cylinder in a deep boundary layer type of incident shear flow (29). The photograph was provided by Dr. John F. Howell, University of Bath, England.

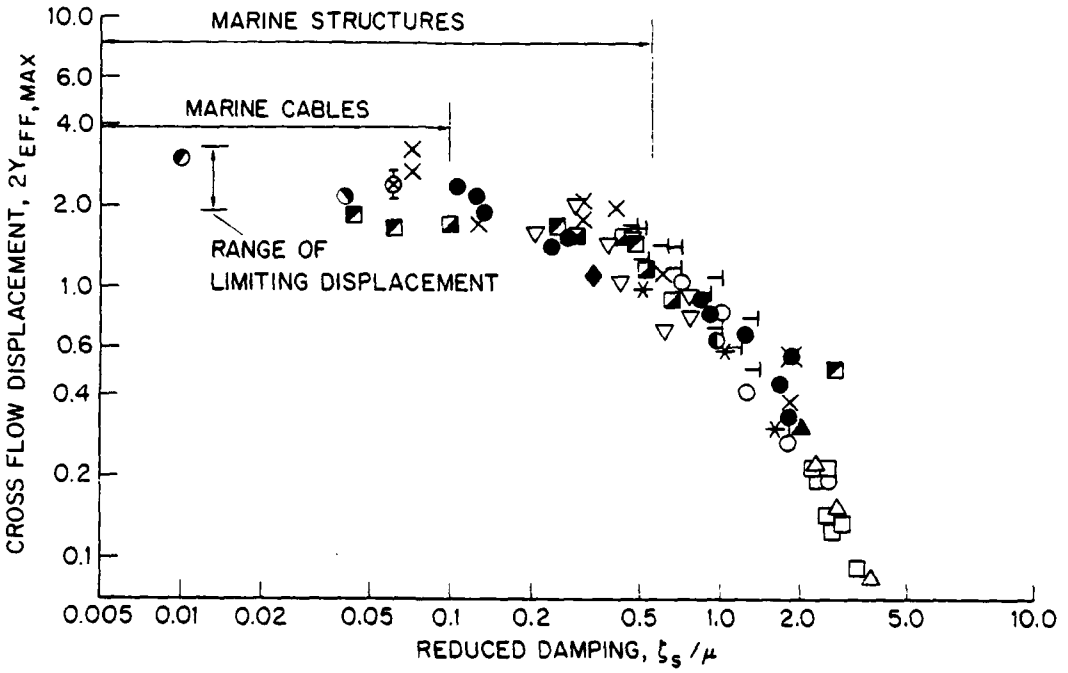

Figure A1. Maximum vortex-excited cross flow displacement amplitude $2Y_{EFF,MAX}$ of circular cylinders, scaled as in equation (A.4), plotted against the reduced damping $\zeta_s/\mu = 2\pi St^2(2m\delta/\rho D^2)$. The legend for the data points is given in Table A1.

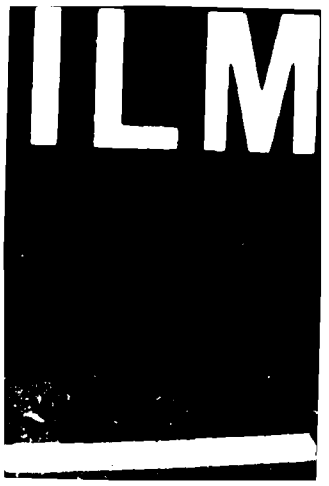
ILM